Electrical resistivity studies on $Zr_xTb_{1-x}Fe_3$ (*x* = 0.2, 0.3) hydrides

# Electrical resistivity studies on $Zr_xTb_{1-x}Fe_3$ ($x = 0.2$, 0.3) hydrides

**R Sivakumar, S Ramaprabhu[1] and K V S Rama Rao**

Alternative Energy, Magnetism and Magnetic Materials Laboratory, Department of Physics,
Indian Institute of Technology, Madras—600 036, India

E-mail: ramp@mmm.iitm.ernet.in

## Abstract

The hydrogen absorption isotherm at 30 °C in the range $0.2 \leqslant P$ (bar) $\leqslant 20$ for $Zr_{0.2}Tb_{0.8}Fe_3$ and $Zr_{0.3}Tb_{0.7}Fe_3$ shows the presence of $\alpha$, $(\alpha + \beta)$ and $\beta$ phases. The study of the kinetics of hydrogen absorption in $Zr_{0.2}Tb_{0.8}Fe_3$ at 30 °C as a function of pressure in the range $8 \leqslant P$ (bar) $\leqslant 50$ shows the presence of different phases. The dependence of the electrical resistivity ($\rho$) on the hydrogen concentration in the $Zr_{0.2}Tb_{0.8}Fe_3$–H and $Zr_{0.3}Tb_{0.7}Fe_3$–H systems is discussed on a basis of the combined effects of depopulation of conduction electrons and formations of various phases, namely $\alpha$, $\alpha + \beta$ and $\beta$. Changes in the slopes of the plots of $\rho$ against $y$ indicate the different phase regions.

## Nomenclature

| | |
|---|---|
| $P$–$C$ isotherm | Pressure–composition isotherm |
| $\alpha$ | First single-phase region of the $P$–$C$ isotherm |
| $\beta$ | Second single-phase region of the $P$–$C$ isotherm |
| $(\alpha + \beta)$ | Plateau region (mixed phase) of the $P$–$C$ isotherm |
| $P_{\alpha \rightarrow \beta}$ | Plateau pressure (bar) |
| $\xi$ | Ratio of the amount of material reacted with $H_2$ to total amount of material |
| $t$ | Reaction time |
| $T$ | Absolute temperature |
| $y$ | Hydrogen concentration (No of H atoms/f.u. of the material) |
| $\Delta V / V$ | Relative volume expansion of the unit cell |
| $\rho$ | Electrical resistivity |

## 1. Introduction

In a metal–hydrogen system, the pressure–composition–temperature ($P$–$C$–$T$) relations show single phases ($\alpha$, $\beta$) and two-phase ($\alpha + \beta$) regions. These phases and phase regions, shown in the isotherms, can also be identified from studies of the dependence of the thermodynamical

---

[1] Corresponding author.

parameters ($\Delta H_H$ and $\Delta S_H$) on hydrogen concentration and from the kinetics of hydrogen absorption. Recently, the hydrogen solubility properties of $Zr_xTb_{1-x}Fe_3$ ($x = 0.1, 0.2, 0.3$) and $Zr_xTb_{1-x}Fe_{1.5}Co_{1.5}$ ($x = 0.1, 0.2, 0.3$) systems have been studied. The presence of $\alpha$, ($\alpha + \beta$) and $\beta$ phases have been identified using two different techniques, namely (i) from the dependence of $\Delta H_H$ and $\Delta S_H$ on the hydrogen concentration and (ii) from kinetics studies by fitting the experimental data to a second-order equation [1–4].
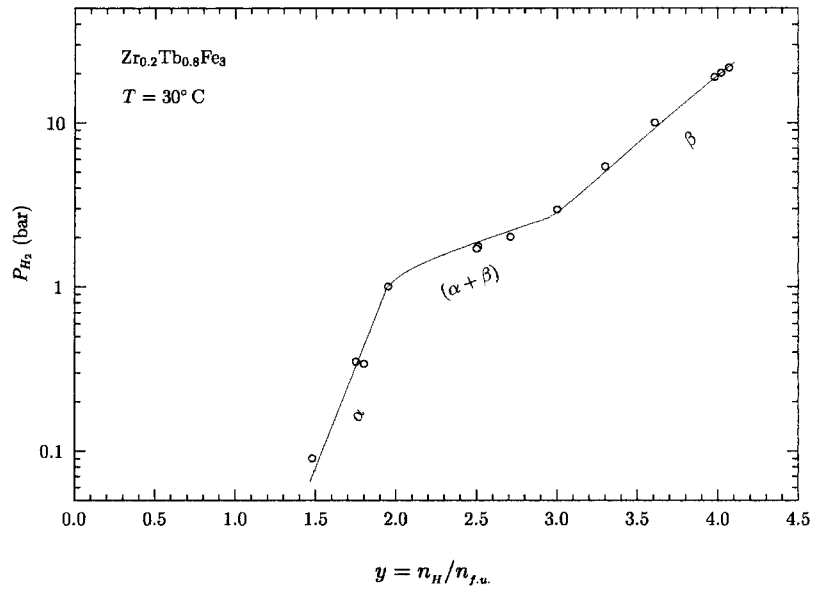


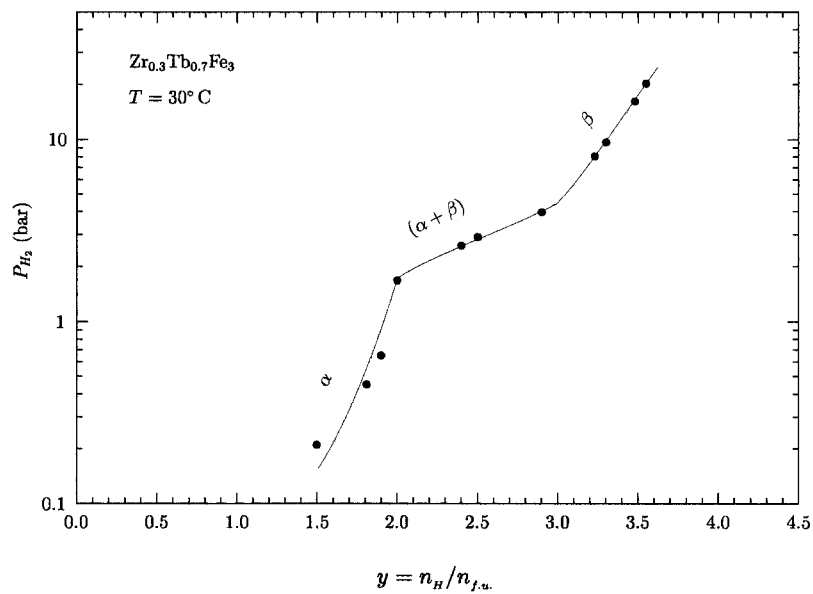**Figure 1.** The hydrogen absorption $P$–$C$ isotherm of $Zr_{0.2}Tb_{0.8}Fe_3$ at 30 °C.



**Figure 2.** The hydrogen absorption $P$–$C$ isotherm of $Zr_{0.3}Tb_{0.7}Fe_3$ at 30 °C.

Occlusion of hydrogen in the host matrix modifies the electrical properties. The electrical properties of the hydrides are not fully understood because it is experimentally difficult to prepare bulk fracture-free hydrides following hydrogenation. In general, the fracture occurs as a result of a large and rapid expansion of the crystal. For instance, the volume expansion is about 20% in going from $LaNi_5$ and $LaNi_5H_6$. Some investigations have tried to overcome this difficulty by using compressed powder [5, 6] or thin films [7, 8]. From electrical resistivity studies on compressed powders, one can gain qualitative information with regard to the dependence of the resistivity on the hydrogen concentration, but the real resistivity of a bulk hydride cannot be obtained due to the presence of grain boundaries. The results obtained from thin-film samples, on the other hand, may give the real resistivity, but the values of the resistivity so obtained need not necessarily be the same as that obtained using crystalline bulk hydride. Electrical resistivity measurements have been recently carried out on single-crystal hydrides [9], and an *in situ* method has been used in the case of polycrystalline $LaNi_5$–H and $LaCo_5$–H systems [10]. For the case of the $Zr_{1-x}Ho_xCo_2$ ($0 \leqslant x \leqslant 1$) system, for which $P$–$C$–$T$ relations and kinetics studies have been reported [11–13], the temperature variations of the electrical resistivity curves of the hydrides of $Zr_{1-x}Ho_xCo_2$ have been discussed in terms of metal–semiconductor transitions [5].
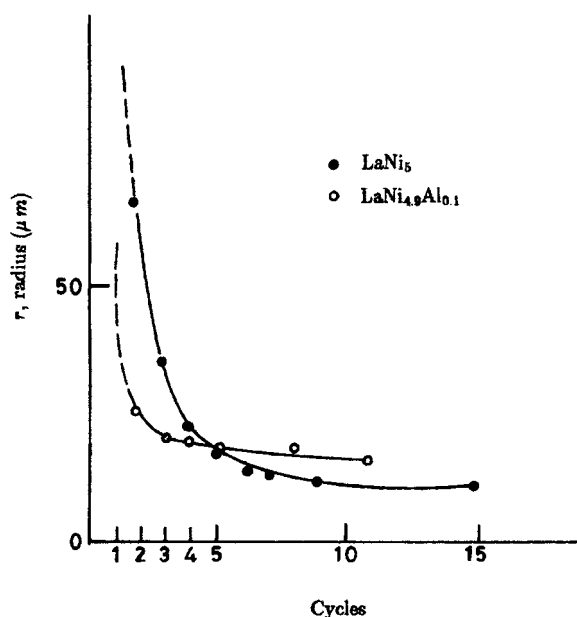


**Figure 3.** The dependence of the particle size on the number of hydrogen absorption–desorption cycles in $LaNi_5$ and $LaNi_{4.9}Al_{0.1}$ [14].

In the present investigation, in order to study the effect of increase in hydrogen concentration on the electrical resistivity, variation of the electrical resistivity as a function of hydrogen concentration has been carried out for $Zr_{0.2}Tb_{0.8}Fe_3$–H and $Zr_{0.3}Tb_{0.7}Fe_3$–H systems at 30 °C. The measurements of the resistivity as a function of hydrogen concentration have been performed on alloy hydride pellets, using a four-probe van der Pauw method at 30 °C.

## 2. Experimental details

The preparation and characterization of $Zr_{0.2}Tb_{0.8}Fe_3$ and $Zr_{0.3}Tb_{0.7}Fe_3$ alloys have been presented in an earlier communication [1, 2]. The hydrogen absorption isotherms and kinetics studies were carried out using a high-pressure hydrogen absorption set-up based on a Sieverts-type apparatus [4]. Before taking equilibrium measurements, the alloys were activated for hydrogen absorption as mentioned in [1].
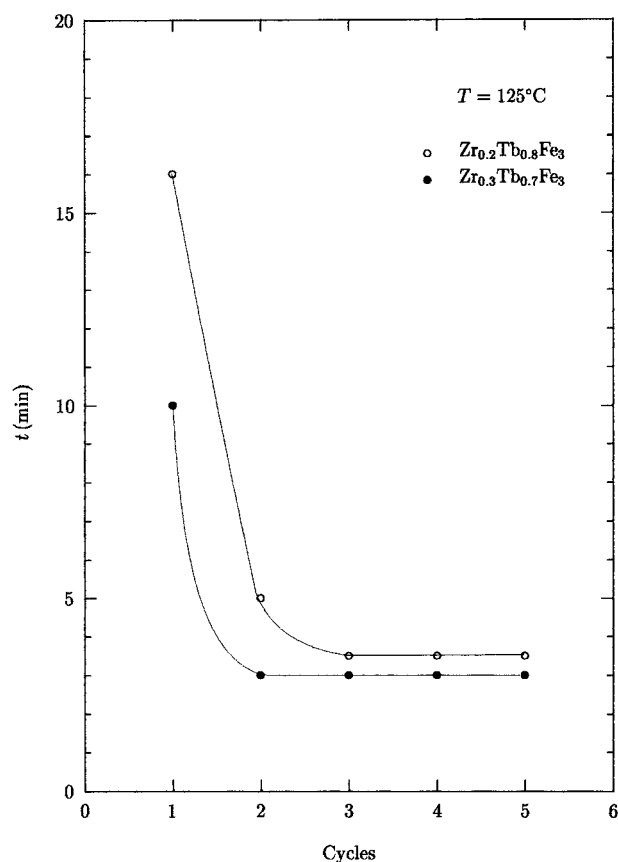


**Figure 4.** The dependence of the time required to reach equilibrium on the number of cycles in $Zr_{0.2}Tb_{0.8}Fe_3$ and $Zr_{0.3}Tb_{0.7}Fe_3$.

## 3. $P$–$C$ isotherms at 30 °C

The $P$–$C$ isotherms for $Zr_{0.2}Tb_{0.8}Fe_3$ and $Zr_{0.3}Tb_{0.7}Fe_3$ obtained in the pressure range $0.1 \leqslant P$ (bar) $\leqslant 25$ at 30 °C are shown in figures 1 and 2 respectively. It can be seen from these isotherms that the maximum hydrogen intake capacity for $Zr_{0.3}Tb_{0.7}Fe_3$ is lower than that for $Zr_{0.2}Tb_{0.8}Fe_3$ and the plateau pressure for $Zr_{0.3}Tb_{0.7}Fe_3$ alloy is higher than that for $Zr_{0.2}Tb_{0.8}Fe_3$. The observed effects can be explained by the smaller unit-cell volume of $Zr_{0.3}Tb_{0.7}Fe_3$ due to the higher Zr content as compared to that of $Zr_{0.2}Tb_{0.8}Fe_3$. The $P$–$C$ isotherms of $Zr_{0.2}Tb_{0.8}Fe_3$ and $Zr_{0.3}Tb_{0.7}Fe_3$ show the $\alpha$, $(\alpha + \beta)$ and $\beta$ phases and these are labelled on the isotherms (figures 1 and 2). In both cases, the $\alpha$ phase extends over the hydrogen

concentration range 1.5–2.0 and the ($\alpha + \beta$) phase over 2–3 hydrogen atoms per formula unit, beyond which the $\beta$ phase exists. The maximum hydrogen intake capacity in $Zr_{0.3}Tb_{0.7}Fe_3$ is lower than that of $Zr_{0.2}Tb_{0.8}Fe_3$ at any particular pressure due to the higher Zr content in $Zr_{0.3}Tb_{0.7}Fe_3$.
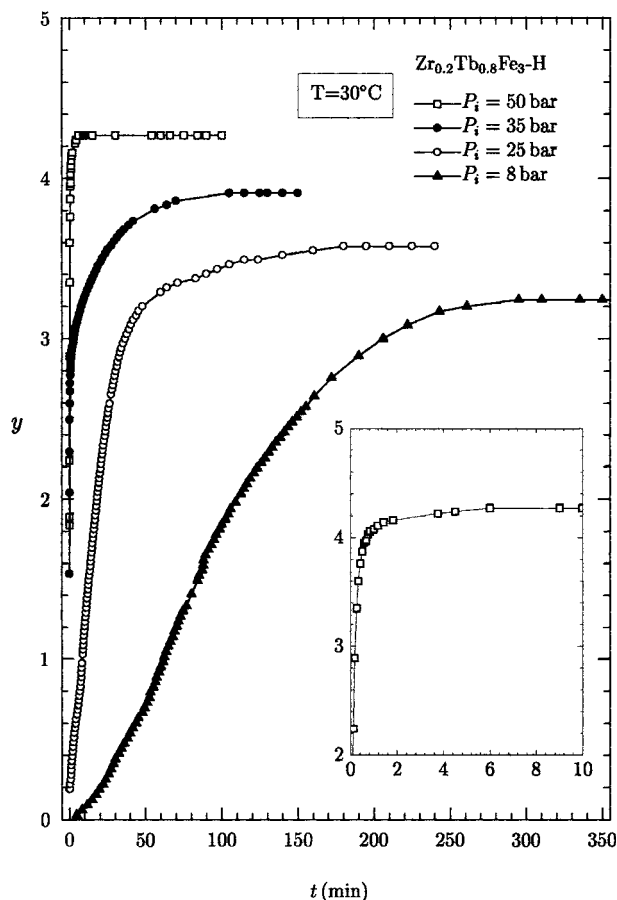


**Figure 5.** The kinetics of hydrogen absorption in the $Zr_{0.2}Tb_{0.8}Fe_3$ system as a function of the hydrogen pressure at 30 °C.

## 4. Electrical resistivity measurements

### 4.1. Preparation of alloy hydrides

In order to measure the electrical resistivity ($\rho$) by a four-probe technique, samples are generally prepared in the form of pellets. Because alloy hydrides are in the form of powders, samples for the measurement of $\rho$ have been prepared as compressed pellets (about 10 tonn cm$^{-2}$). In the present study; uniformity of particle size has been achieved by the complete activation treatment of $Zr_{0.2}Tb_{0.8}Fe_3$ and $Zr_{0.3}Tb_{0.7}Fe_3$. Initially, the parent alloy (ingot) was activated for hydrogen absorption by carrying out several absorption–desorption cycles. In the first cycle of absorption and desorption, the alloy ingot breaks into small pieces through the formation of cracks. Further hydrogen absorption–desorption cycling leads to a reduction of particle size

which reaches a minimum saturation value beyond which cycling does not have any effect on the particle size. The relation between the rate of hydrogen absorption and the number of cycles is such that when the time required for two consecutive absorption cycles is the same then the activation is complete. Thereafter, the particle size remains uniform.
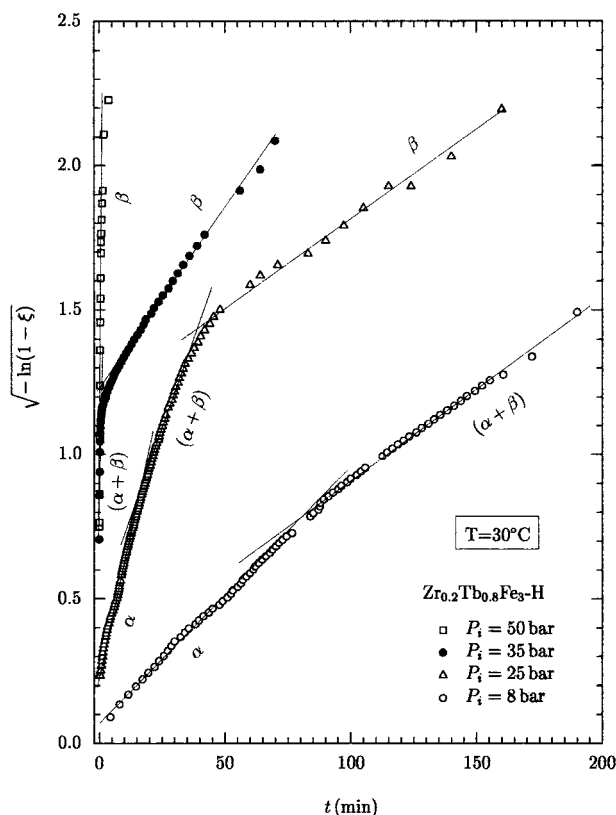


**Figure 6.** The kinetics data (as a function of pressure at 30 °C) fitted to a second-order rate equation for the $Zr_{0.2}Tb_{0.8}Fe_3$–H system.

Figure 3 shows the relationship between the radius ($r$ ($\mu$m)) of the alloy hydride particles and the number of hydrogen absorption–desorption cycles for the case of $LaNi_5$ and $LaNi_{4.9}Al_{0.1}$ alloys at 298 K [14]. It can be observed from figure 3 that for $LaNi_5$, a minimum of about 10–15 cycles is necessary to attain a uniform particle size, whereas for $LaNi_{4.9}Al_{0.1}$ only about 7–10 hydrogen absorption–desorption cycles are required. For the present systems, the dependence of the time required to reach equilibrium on the number of cycles for $Zr_{0.2}Tb_{0.8}Fe_3$–H and $Zr_{0.3}Tb_{0.7}Fe_3$–H is shown in figure 4, and it has been found that 2–3 absorption–desorption cycles are sufficient to completely activate the alloys at 125 °C.

The hydrides of $Zr_{0.2}Tb_{0.8}Fe_3$ and $Zr_{0.3}Tb_{0.7}Fe_3$ have been prepared with various hydrogen concentrations by allowing the alloy to react with hydrogen at different known hydrogen pressures. The hydride powders were then pelletized to a size of 8 mm diameter and approximately 1 mm thickness. The densities of all the hydride pellets have been measured and the deviation from the mean value did not vary by more than 7%.

## 5. Absorption kinetics at 30 °C

The studies of the kinetics of hydrogen absorption at room temperature (30 °C) were carried out for $Zr_{0.2}Tb_{0.8}Fe_3$ alloy as a function of pressure in the range $8 \leqslant P$ (bar) $\leqslant 50$ and the results are shown in figure 5. The rate of hydrogen absorption has been found to increase with increasing hydrogen gas pressure. When the rate is fitted to a second-order equation, the curves are transformed to different straight lines corresponding to different phases of the alloy hydrides as seen from figure 6. The concentrations at which the slope changes correspond to the different phase boundaries ($\alpha \rightarrow (\alpha + \beta)$, $(\alpha + \beta) \rightarrow \beta$) as marked in these figures. The different possible rate-determining steps involved in the hydrogen absorption kinetics are the surface process, the interface process and diffusion.
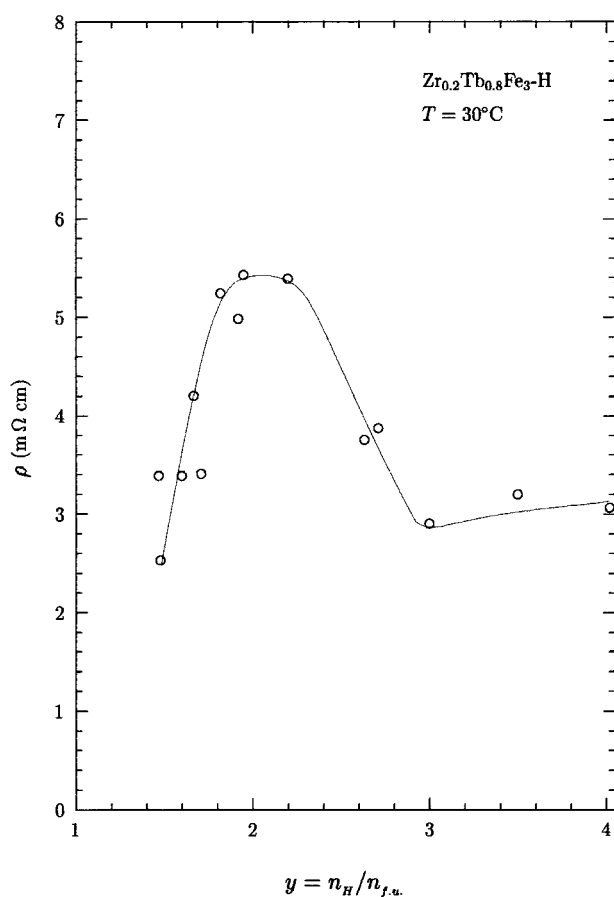


**Figure 7.** The variation of the electrical resistivity with the hydrogen concentration in the $Zr_{0.2}Tb_{0.8}Fe_3$–H system.

## 6. Results and discussion

The electrical resistivities of the alloy hydrides have been obtained by van der Pauw four-probe method. Figures 7 and 8 show the variation of electrical resistivity ($\rho$) with hydrogen concentration ($y$) for $Zr_{0.2}Tb_{0.8}Fe_3$–H and $Zr_{0.3}Tb_{0.7}Fe_3$–H respectively.
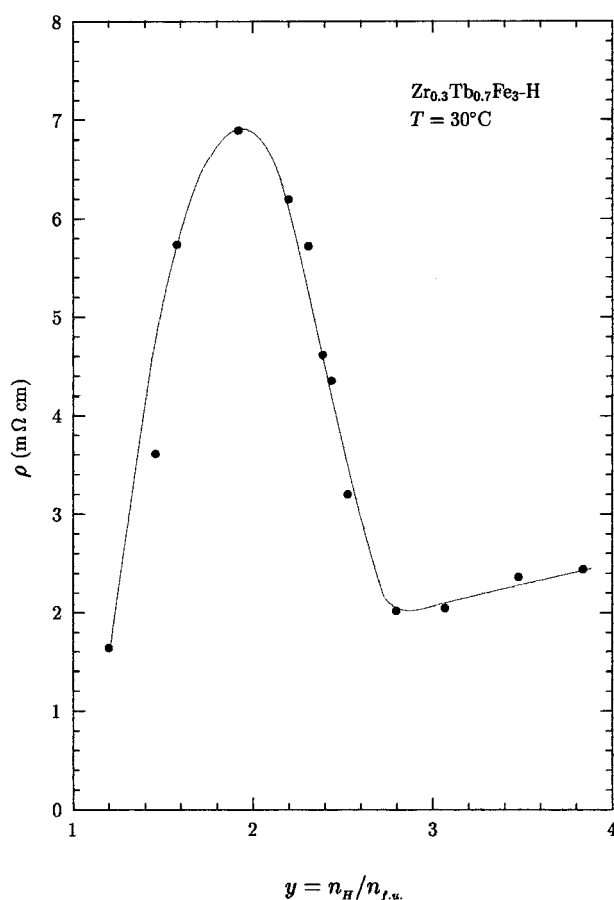
**Figure 8.** The variation of the electrical resistivity with the hydrogen concentration in the $Zr_{0.3}Tb_{0.7}Fe_3$–H system.

Figures 7 and 8 show that there is a steep increase in resistivity with increasing hydrogen concentration up to about $y = 1.8$ to $2.0$, where there is a decrease in resistivity up to about $y = 2.8$ to $2.9$ and, then, there is again an increase in $\rho$ with increasing hydrogen content. These observations could be explained with the help of the formation of various phases in an alloy hydride system. Figure 9 shows a schematic representation of the formation of $\alpha$, $(\alpha + \beta)$ and $\beta$ phases starting from the parent alloy. Initially, as the hydrogen gas molecules approach the surface of the alloy, physisorption and then chemisorption take place with the dissociation of $H_2$ molecules into H atoms at the surface. In the $\alpha$ phase, the hydrogen atoms occupy randomly the available interstitial sites to form a solid solution. Random occupations of hydrogen atoms act as scattering centres for the conduction electrons, and hence increase the resistivity. In addition, it has been shown that in the case of R–Fe systems, the addition of hydrogen atoms is accompanied by a decrease in conduction electron density [15–17]. This depopulation of s-electron density will further increase the resistivity. In essence, there is an increase in resistivity in the region of the $\alpha$ phase.

A further increase in hydrogen concentration results in H–H attractive interaction, leading to the formation of clusters. Hence the two-phase $(\alpha + \beta)$ region condenses as illustrated in figure 9. Even though there is a decrease of s-electron density, the formation of clusters
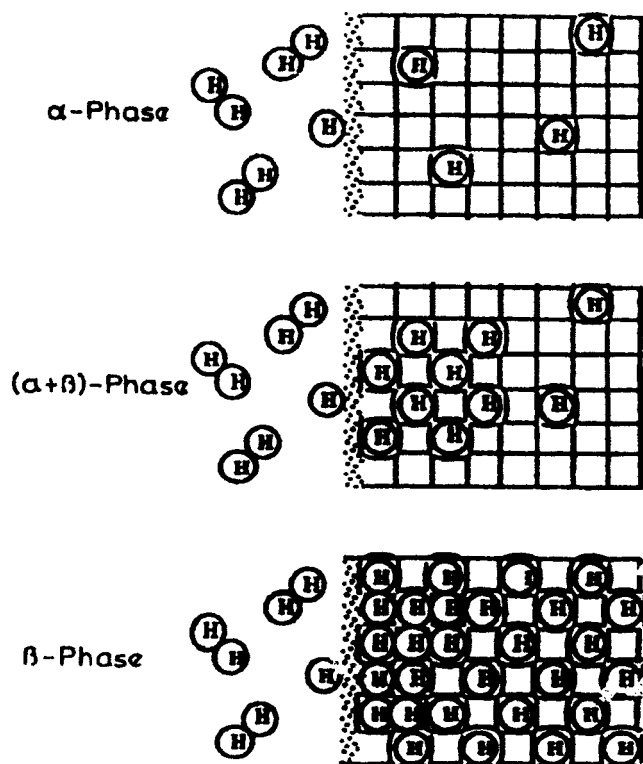
**Figure 9.** A schematic diagram showing the formation of $\alpha$, ($\alpha + \beta$) and $\beta$ phases in an alloy–hydrogen system.

leads to a decrease in the effective number of scattering centres because each cluster now acts as a single scattering centre and, as the current always takes the path of least resistance, conduction becomes possible. Therefore, a net decrease in resistivity is observed. Addition of more hydrogen atoms beyond the ($\alpha + \beta$) $\rightarrow$ $\beta$ phase boundary region leads to the precipitation of hydride phase ($\beta$), where the hydrogen atoms randomly occupy positions in the alloy hydride causing the scattering centres once again to increase with increase in hydrogen concentration. Thus, in the $\beta$ phase, a net increase in resistivity is observed. The $\rho$ versus $y$ plots (figures 7 and 8) therefore show the existence of different phases in the $Zr_{0.2} Tb_{0.8} Fe_3$–H and $Zr_{0.3} Tb_{0.7} Fe_3$–H systems. In the case of the $LaNi_5$–H and $LaCo_5$–H systems, it has been shown from the pressure dependence of the resistivity that the change in resistivity corresponds to a transformation between $\alpha$ and $\beta$ phases [10].

## Acknowledgments

## References

[1]  Sivakumar R, Ramaprabhu S, Rama Rao K V S, Anton H and Schmidt P C 1999 *J. Alloys Compd.* **285** 143
[2]  Sivakumar R, Ramaprabhu S, Rama Rao K V S, Anton H and Schmidt P C 2000 *Int. J. Hydrogen Energy* 463

 [3] Sivakumar R, Ramaprabhu S, Rama Rao K V S, Mayer B and Schmidt P C 2000 *J. Alloys Compd.* **302** 146
 [4] Sivakumar R, Ramaprabhu S, Rama Rao K V S, Mayer B and Schmidt P C 1999 *Int. J. Hydrogen Energy.* accepted for publication
 [5] Ramesh R and Rama Rao K V S 1994 *J. Appl. Phys.* **76** 3556
 [6] Annapoorni S, Markandeyulu G and Rama Rao K V S 1990 *J. Phys. Soc. Japan* **59** 3014
 [7] Adachi G, Niki K, Nagai H and Shiokawa J 1985 *J. Less Common Met.* **108** 107
 [8] Sakaguchi H, Yagi Y, Taniguchi N, Adachi G and Shiokawa J 1987 *J. Less Common Met.* **135** 137
 [9] Bartashevich M I, Goto T and Yamaguchi M 1992 *J. Magn. Magn. Mater.* **111** 83
[10] Ishikawa F, Tega H, Yamamoto I and Yamaguchi M 1995 *J. Alloys Compd.* **231** 182
[11] Ramesh R, Annapoorni S and Rama Rao K V S 1991 *J. Less Common Met.* **170** 75
[12] Ramesh R and Rama Rao K V S 1993 *J. Alloys Compd.* **191** 101
[13] Ramesh R, Murti Y V G S, Reddy K V, Rama Rao K V S and Das T P 1994 *J. Alloys Compd.* **205** 211
[14] Rudman P S 1983 *J. Less Common Met.* **89** 93
[15] Buschow K H J and Sherwood R C 1978 *J. Appl. Phys.* **49** 1480
[16] Annapoorni S and Rama Rao K V S 1990 *J. Appl. Phys.* **67** 424
[17] Cohen R L, West K W, Oliver F and Buschow K H J 1980 *Phys. Rev.* B **21** 941